



Capacity for Rail

***Towards an affordable, resilient, innovative
and high-capacity European Railway
System for 2030/2050***

Report from on-track
demonstrations

Submission date: 29/11/2017

Deliverable 55.4

*This project has received funding
from the European Union's
Seventh Framework Programme
for research, technological
development and demonstration
under grant agreement n° 605650*



Collaborative project SCP3-GA-2013-60560
Increased Capacity 4 Rail networks through
enhanced infrastructure and optimised operations
FP7-SST-2013-RTD-1

Lead contractor for this deliverable:

- ADIF

Project coordinator

- Union Internationale des Chemins de fer, UIC

Executive Summary

The CAPACITY4RAIL project will provide research activities in the areas of infrastructure, rolling stock, operations and monitoring techniques. These research tasks will be covered with several demonstrators that will be carried out in different environments (laboratory facilities, virtual environment and on track). These demonstrators will enable the assessment of the innovations developed in the project.

The main objectives of this WP55 – Demonstration, evaluation and assessment are:

- To carry out test-scale demonstrations on infrastructure or in laboratories or demonstrations in virtual environment of the innovations proposed in the different subprojects.
- To evaluate the technical results of the demonstrations.
- To combine these results with the scenarios evaluation to perform a global assessment of the innovations proposed in the project.
- To perform safety and risk assessment for the demonstrators according to CSM.

This document D5.5.4 will describe the selected demonstrations performed on infrastructure. The test sites will be configured for each of the demonstrations according to the Test Plans.

The total budget of the Demonstrators is 1.895.633 € including the costs of Coordination-Planning-Report-Assessment.

The following is the complete list of demonstrators.

| SP | WP | |
|---|-------|--|
| DEM of new prototypes of Slab Track; LAB-Rail track accelerated testing at CEDEX (1:1 scale) | | |
| 1 | 1.1 | <i>Demo of new prototype of Slab Track (1st prototype)</i> |
| 1 | 1.1 | <i>Demo of new prototype of Slab Track (2nd prototype)</i> |
| | | <i>Related task</i> |
| 1 | 1.1.3 | <i>Full design of prototypes of new concepts for infrastructures</i> |
| 1 | 1.1 | <i>Lab-testing of a innovative rail section</i> |
| | 4.3 | <i>Real-scale tests of embedded RFID sensor tags (with SP1 - CEDEX) - Later</i> |
| VHST | | |
| 1 | 1.2 | <i>DEM-Laboratory, Track for VHS very high speed; Rail track accelerated testing</i> |
| 1 | 1.2 | <i>Other DEM-activity/task associated: DEM-Full scale testing of an existing bridge susceptible to high vibrations</i> |
| Switches and crossing | | |
| 1 | 1.3 | <i>Decisions tool for S&C maintenance based on track recording car information</i> |
| 1 | 1.3 | <i>Using wireless technology to S&C monitoring</i> |
| 1 | 1.3 | <i>New material for S&C crossing in service</i> |
| 1 | 1.3 | <i>Material validation data for wear map</i> |
| 1 | 1.3 | <i>Laser measurements of S&C frog nose</i> |
| 1 | 1.3 | <i>Innovative technology to remove snow in turnouts</i> |
| Embebbed RFID + Innovative monitoring sensors | | |
| 4 | 4.3 | <i>In-lab tests of embedded RFID sensor tags</i> |
| 4 | 4.3 | <i>Real-scale tests of embedded RFID sensor tags (with SP1 - CEDEX)</i> |
| 4 | 4.3 | <i>Lab demonstration of innovative monitoring sensors</i> |
| 4 | 4.3 | <i>Real scale tests of innovative monitoring sensors</i> |
| DEM of retro-fitting | | |
| 4 | 4.4 | <i>In-lab and on-track validation tests</i> |
| DEM-Virtual reality | | |
| 5 | 5.5.5 | <i>DEM-Virtual reality; Impact of new technologies developed in the project.</i> |
| Other DEM | | |
| 5 | 5.5 | <i>DEM-Coordination-Planning-Report-Assessment</i> |

Table of contents

| | |
|--|----|
| Executive Summary | 3 |
| Table of contents | 5 |
| 1. Background..... | 6 |
| 2. Objectives | 7 |
| 3. On- Track Demonstrations | 8 |
| 3.1.Battery driven wireless sensors for S&C | 8 |
| 3.2. Marketable retro-fit kits. Monitoring use case (Alcácer do Sal Railway Bridge)..... | 12 |
| 3.3. New crossing material..... | 29 |
| 3.4 Data collection during in-situ test campaigns | 39 |
| 3.5. Innovative designs and methods of structures on very high speed lines. | 42 |
| 4. Conclusions..... | 47 |
| 5. References..... | 49 |

1. Background

CAPACITY4RAIL project will deliver technological innovations that will contribute towards the achievement of 2030/2050 EU targets. The project has a cross-cutting approach and provides research in the areas of infrastructure, rolling stock, operations and monitoring techniques. As a result from the research activity, several demonstrators will be carried out in laboratory at reduced and real scale, virtual environment and on a commercial line.

The demonstrators play a crucial role in CAPACITY4RAIL as they enable the assessment of the innovations developed in the project, which will serve to identify room for improvement and will guide their further development. Moreover, the demonstrators in combination with the scenarios evaluation will enable the global assessment of the step-innovations proposed in CAPACITY4RAIL with regards to the 2030/2050 vision of the European Union, which is required to properly devise the most suitable migration path to meet EU long-term targets.

The role of WP5.5 is to coordinate and develop the demonstrations activities of CAPACITY4RAIL, in collaboration with the partners involved in it.

2. Objectives

The objectives of this deliverable are:

- To carry out test-scale demonstrations on infrastructure of the innovations proposed in the different subprojects
- To evaluate the technical results of the demonstrations
- To combine these results with the scenarios evaluation to perform a global assessment of the innovations proposed in the project
- To perform safety and risk assessment for the demonstrators according to CSM

Selected demonstrations will be performed on infrastructure. The test sites will be configured for each of the demonstrations according to the Test Plans.

3. On- Track Demonstrations

3.1. BATTERY DRIVEN WIRELESS SENSORS FOR S&C

Measurement with battery driven wireless sensor has been tested at Trafikverket. The solution was delivered by Konux and is a commercial available product that still is under development.

Battery lifetime is expected to be at least one year and directly depends on the factors outdoor temperature, number of measurements per day and how often data is transmitted.

The first measurement made in May at Algutsgården has been evaluated and proven to be good both regarding to acceleration values as well as the calculated deflection. After the first test 38 sensors has been installed during the time September 25th – October 12th on totally 4 places in Sweden where it will be evaluated during 2017/2018.

The normal way to decide which maintenance to perform for a turnout (Switch & Crossing, S&C) is to make visual inspections. Track geometry measurements and ultrasonic measurement has been performed over 20 years time, but this information is normally used as if it was the plain line. It is still the manual inspections that still dominate the UIC report.

The most common way to monitor S&C is to measure the motor current when the switch blade is moved and is today a standard way to monitor in some European countries. Another established method in France, Holland and Germany is to measure track geometry, rail profile and take video recording by a train developed to measure in S&C. This is mostly motivated from the aspect to have less people in track and increase the speed of the measurement compared manual inspections.

In some extent acceleration measurement has been introduced over the last decade. Still this field is fairly unexplored. This report gives some basic ideas of a way to use battery equipped wireless sensors that can be deployed on sleepers.

Objectives

The objectives of these demonstrators are to reach a TRL level of 5-6 to enable field test of the concept wireless sensor for measuring train passage in track.

Results

Trafikverket made a tender of 45 wireless sensors in November 2016. The approval was made in February 2017. The company asked to deliver is Konux GmbH in Germany.

A preliminary test was done in May to ensure a delivery in August.

The real delivery was made in end of September with installation at three different stations in Sweden. 28 sensors were deployed in two nights (September 26-27th). Another 13 sensor will be installed October 7th – 12th.

The selected stations are shown in Figure . The track sections between Stockholm-Göteborg/Malmö are the lines with most passenger trains in the country. In Katrineholm the western main line and the southern main line is separated, so some of the chosen turnouts have all trains passing and some just have the trains continuing on the western main line to Göteborg.



FIGURE 1. SELECTED STATIONS FOR TEST OF SENSORS

| Station | Number of S&C | Type of S&C | Speed [km/h] | Traffic [MGT/year] |
|---------------------|---------------|-------------|---|--------------------|
| <u>Katrineholm</u> | 8 | UIC60 | 140 | 10 (79) |
| <u>Algutsgården</u> | 1 | 60E | 130 (will increase later) | 10.5 (51) |
| <u>Höör</u> | 4 | 60E | 200 | 16.5 (107) |
| <u>Stehag</u> | 6 | UIC60 | 200 (Just north of Stehag it is 160 km/h) | 16.5 (107) |

The X2-train passes each hour at the same time, but depending on delays on the route it might differ some minutes. Going north the train has just left Malmö (about 40 km away) most of the trains are

within 6 minutes from the expected time (85 %). Southbound less trains are within 6 minutes (50 %), mostly because they started 500 km away. The distribution for September is shown Figure 2..

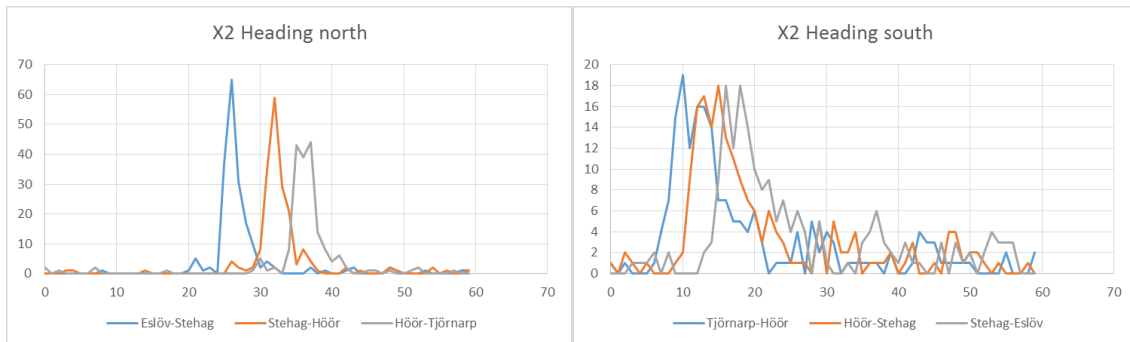


FIGURE 2. DISTRIBUTION WHEN AN X2 TRAIN PASSES A STATION (MINUTES AFTER EACH HOUR) DURING 4 WEEKS IN SEPTEMBER

In Stehag the S&C are of the generation build from about 1990, UIC60. The station was rebuilt in 2012. In Höör the type of S&C are of the latest generation, 60E, that was introduced in 2014. The station was rebuilt in 2014. In all cases the size of the S&C are either radius 760 or 1200 meter.

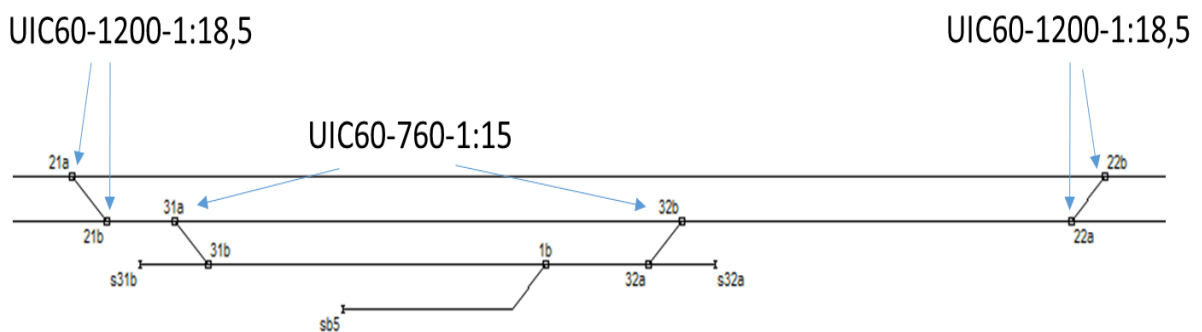


FIGURE 3. STATION STEHAG

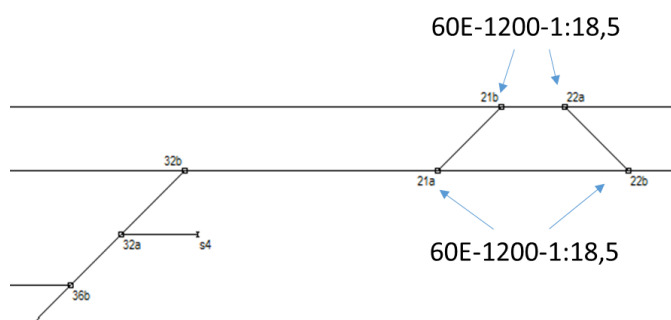


FIGURE 4. STATION HÖÖR

The newer generation of turnout are with rail pads so they are softer and should have less acceleration in the sleepers than the UIC60-generation. The movement of the sleeper can be in the same order as that dependent of the stiffness in the substructure and not the rail pad stiffness.

3.2. MARKETABLE RETRO-FIT KITS. MONITORING USE CASE (ALCÁCER DO SAL RAILWAY BRIDGE)

The Alcácer do Sal Railway Bridge is part of the new Alcácer Railway line, located between Pinheiro station and kilometer (km) 94 of the South Line, which connects Lisbon to the Algarve. The Sado river crossing is located between km 8 + 530 and km 11 + 265 of the variant, with a total development of 2.735 m, consisting of the main bridge and two access viaducts.

The structure is designed for passenger trains with speeds of up to 250 km/h and freight trains with a maximum axle load of 25 tonnes. Figure 15 shows an overview.



FIGURE 5. LOCATION AND GENERAL VIEW OF THE RAILWAY BRIDGE OF ALCÁCER DO SAL

Since several experimental studies have already been conducted in this bridge it has been chosen to implement and test the innovative long-term monitoring system. In this way, two locations were selected as can be seen in Figure 6.

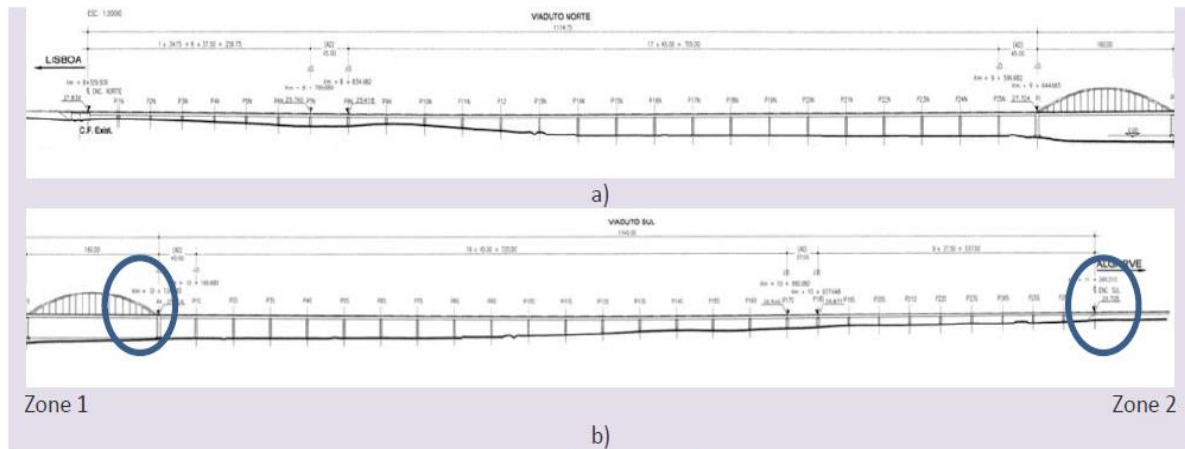


FIGURE 6. LOCATIONS OF MONITORING SYSTEMS

In zone 1, the risk of track buckling and the structural health of one hanger were monitored. In zone 2, the track condition at transition zones were monitored. In each of these locations, it was implemented a long term monitoring system compose by a local main station and two nodes (zone 1) and one node (zone 2). The systems will be described in more detail in the following chapters

MONITORING THE RISK OF TRACK BUCKLING

On a continuous welded rail track, where the expansion of the rails is hardly possible, high compressive stresses occur when there is a significant temperature increase. These compressive stresses may result in track buckling that can be prevented by monitoring the rail temperature and longitudinal strain.

In this way, one sensor node was mounted on the rail aligned with the hanger 51 at zone 1 (Node 1). Figure 17 shows the location in detail. The Node 2 corresponds to the structural health monitoring described in next chapter. Both locations (Node 1 e Node 2) were adopted considering previous studies that have already been carried out in the same alignment and the new data can be compared.

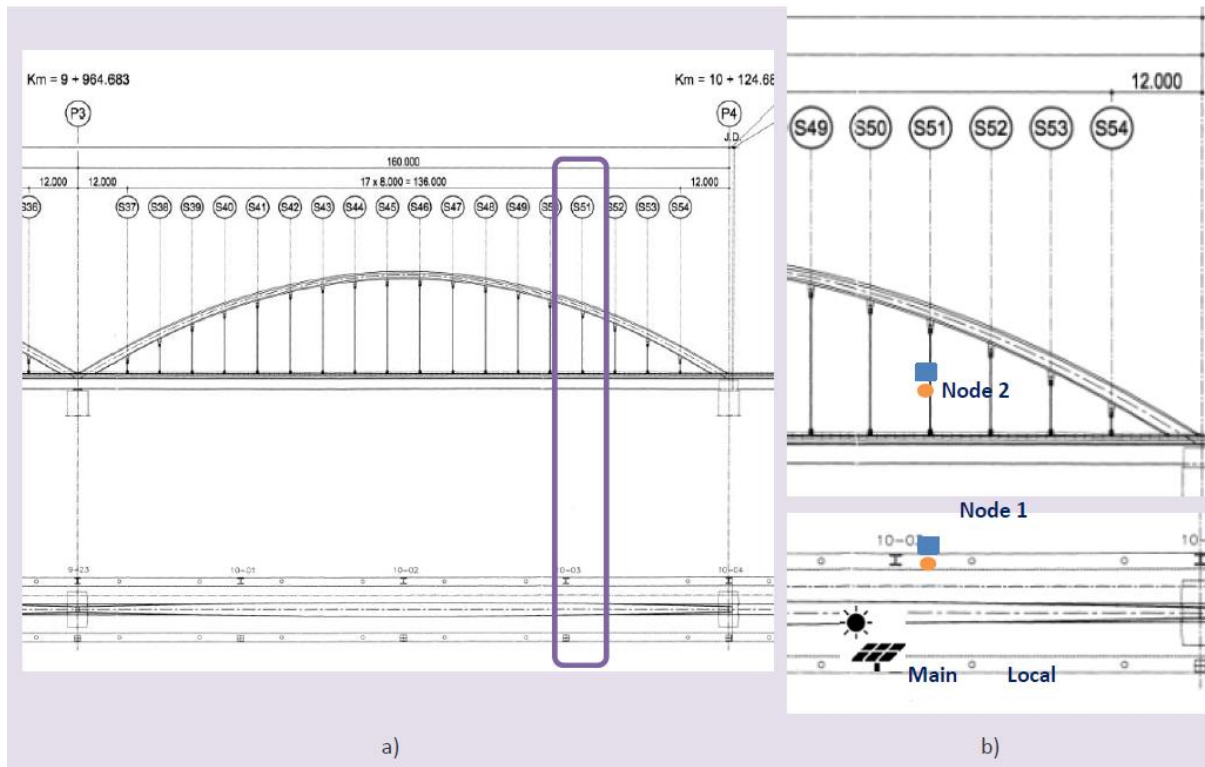


FIGURE 7. EXPERIMENTAL CONFIGURATION AT ZONE 1: A) HANGER ALIGNMENT, B) INSTRUMENTED LOCATIONS

This sensor node includes two weldable strain gages, one temperature sensor (RTD), an energy harvesting module, a ADCs module, a microcontroller and wireless transceiver module, a solar panel and a battery. The sensors were welded (strain gages) and glued (RTD) directly in to the rail and properly protected. The electronic modules were inserted into a small box (125 x 85 x 55 mm) glued to the rail web. The solar panel were fixed in the top of the box. The energy harvesting unit was capable of receiving power from different types of local sources, whoever in this case only a solar panel was installed for generate energy for the sensor node. Figure 18 a) shows the installation illustration and b) the scheme of the node.

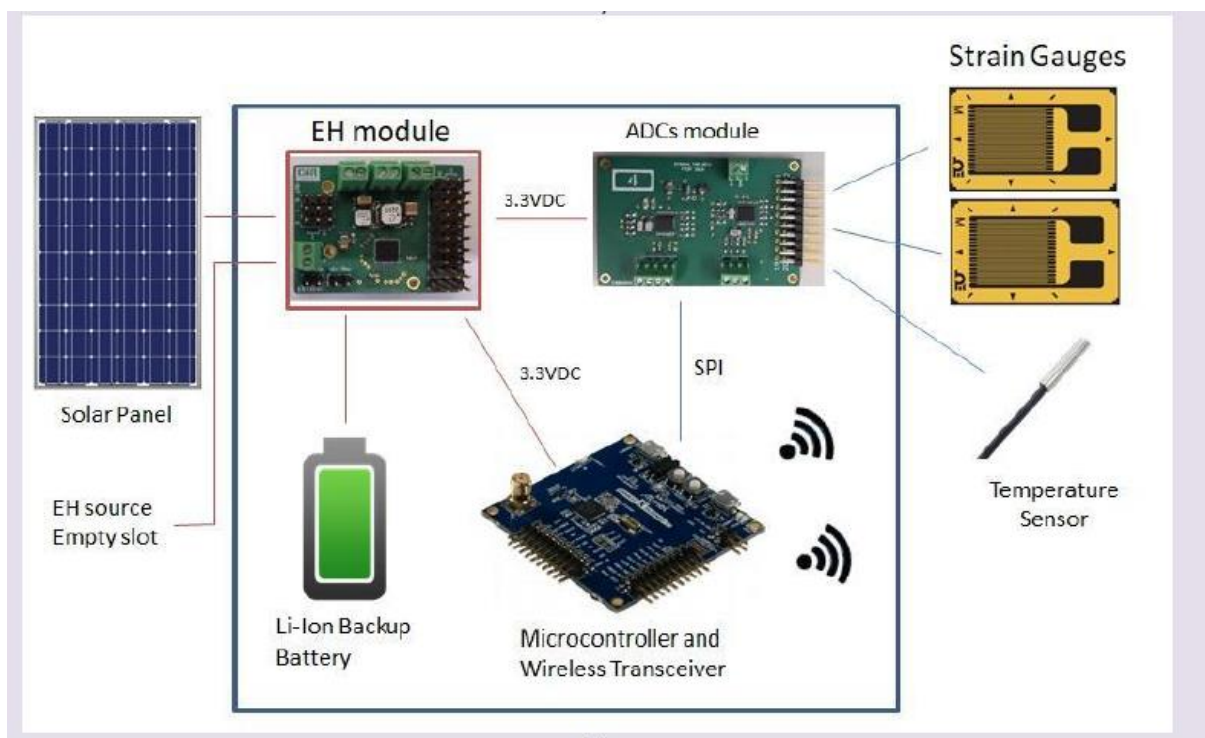


FIGURE 8. SENSOR NODE 1 INSTALLATION A) AND SCHEME B)

To receive the data from the nodes 1 e 2, the main monitoring system (main local station) was installed on the board walk side, opposite at the railroad traffic. A metal structure was developed to hold a solar panel (130W, 1300x655mm) and an industrial enclosure (500x700mm ABS IP65). This structure consisting on a base and a pole was attached to the stud bolts of the catenary posts.

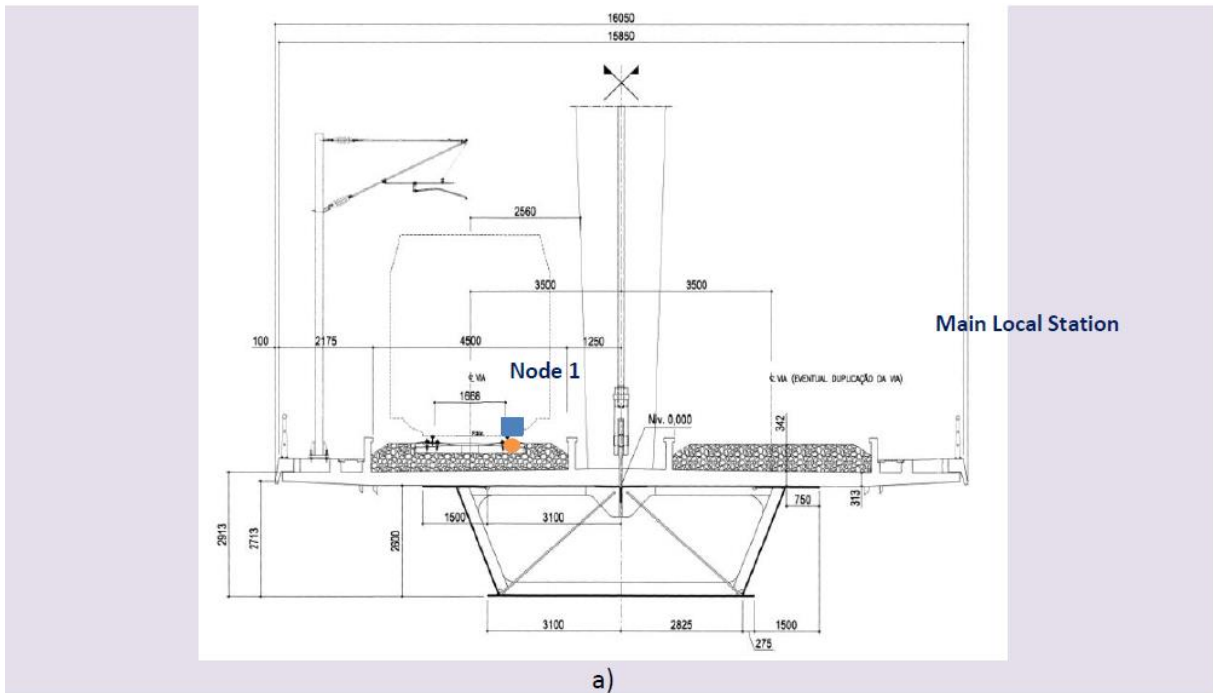




FIGURE 9. LOCATION OF THE MAIN LOCAL STATION A) AND ILLUSTRATION OF INSTALLATION B)

The main local station components are a minicomputer, a node data receiver, a 3G/4G router, a charge controller, a solar panel and 2 batteries, and other auxiliary accessories. Figure 20 shows the system scheme and installation illustration. The node receiver collects the data from node 1 and 2 and saves in a database on the computer which can be accessed via internet.

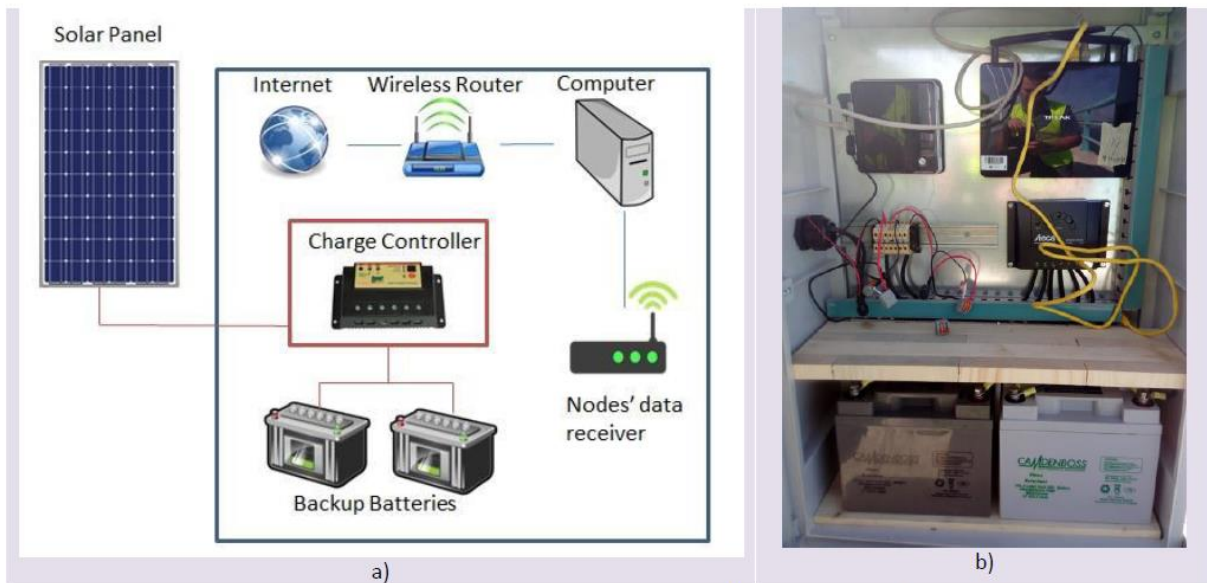


FIGURE 10. MAIN LOCAL STATION AT ZONE 1 SCHEME A) AND ILLUSTRATION B)

STRUCTURAL HEALTH MONITORING OF RAILWAY BRIDGES

The Structural Health Monitoring of a long span railway bridge is important to prevent the failure of critical components of the bridge due to for example fatigue crack propagation.

In this case, a similarly node with the same configuration (to previous case of risk of track buckling – Node 1) was installed on the hanger S51 (Node 2) at zone 1, but now to study the vertical strains/forces of the hanger. Two strain gages, one temperature sensor (RTD), an energy harvesting unit, a ADCs module, a wireless transceiver module, a solar panel and a battery was also used (Figure 18). The installation process was the same instead of the strain gages that were glued in this case.

The node was installed at 2.7 m from the hanger base and the box, with the fixed solar panel, oriented to the maximum solar incidence. Besides of using only the panel solar, the energy harvesting unit was also capable of receiving power from different types of local sources. The main local station to receive the data from Node 2 was the same used for Node 1. In Figure 21 a) it can be seen the scheme of Node 2 and main local station location and b) there illustration.

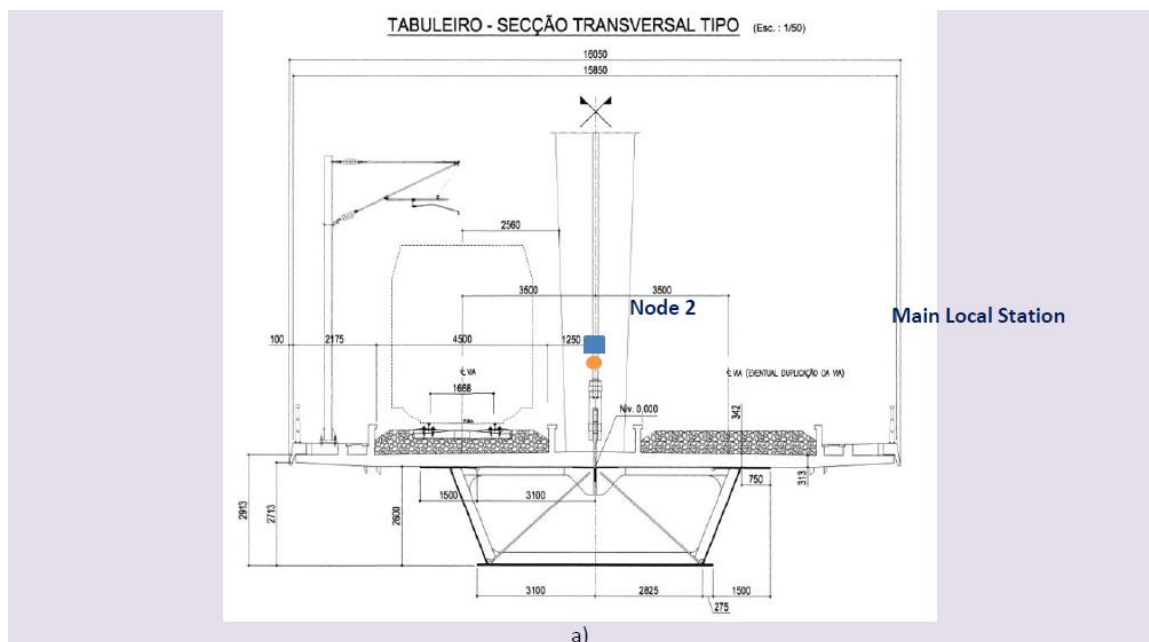


FIGURE 11. LOCATION OF THE NODE 2 A) AND ILLUSTRATION OF INSTALLATION B)

TRACK CONDITION MONITORING AT RAILWAY TRANSITION ZONES

The variation in the subsoil stiffness when changing from one structure to another produce greater stress on the infrastructure. These differences along with the uneven settlement (as “Bump’s” and “Dip’s”, Figure 22) might increase the dynamic loads on the railway components and put in risk the traffic safety.

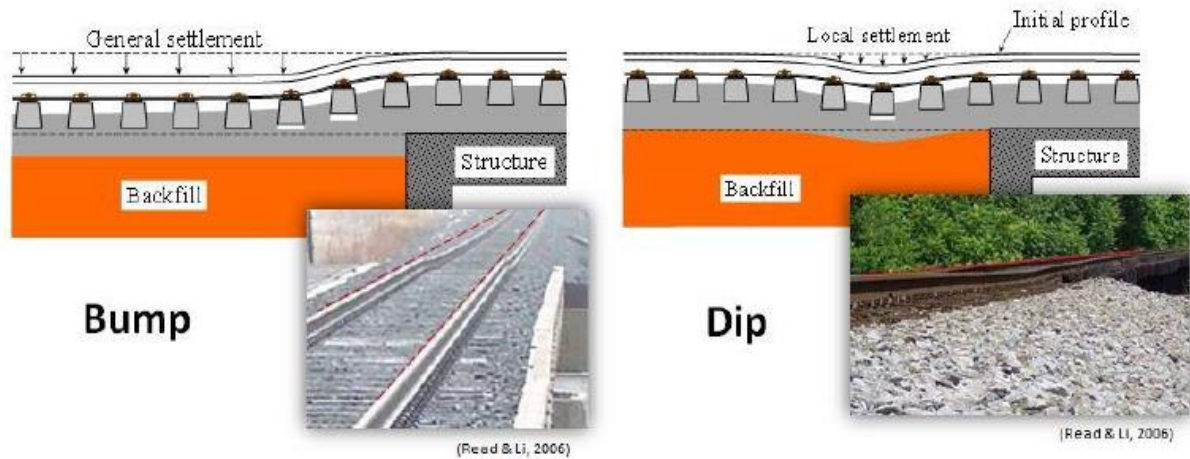


FIGURE 12 – TRANSITION ZONES SETTLEMENTS: GENERAL A) AND LOCAL B)

To study these settlements a several measurements can be taken as sleeper accelerations, rail-sleeper relative displacements, rail and sleeper vertical displacements, wheel loads and rail seat loads. Short term monitoring with this measurements was already conducted in the transition of Zone 2 in the south access viaduct of Alcácer do Sal Railway Bridge, Figure 13). In this way this location was adopted to install the new long term monitoring system for transition zones. A sensor node was installed in a sleeper in the end of the transition zone to measure the accelerations.

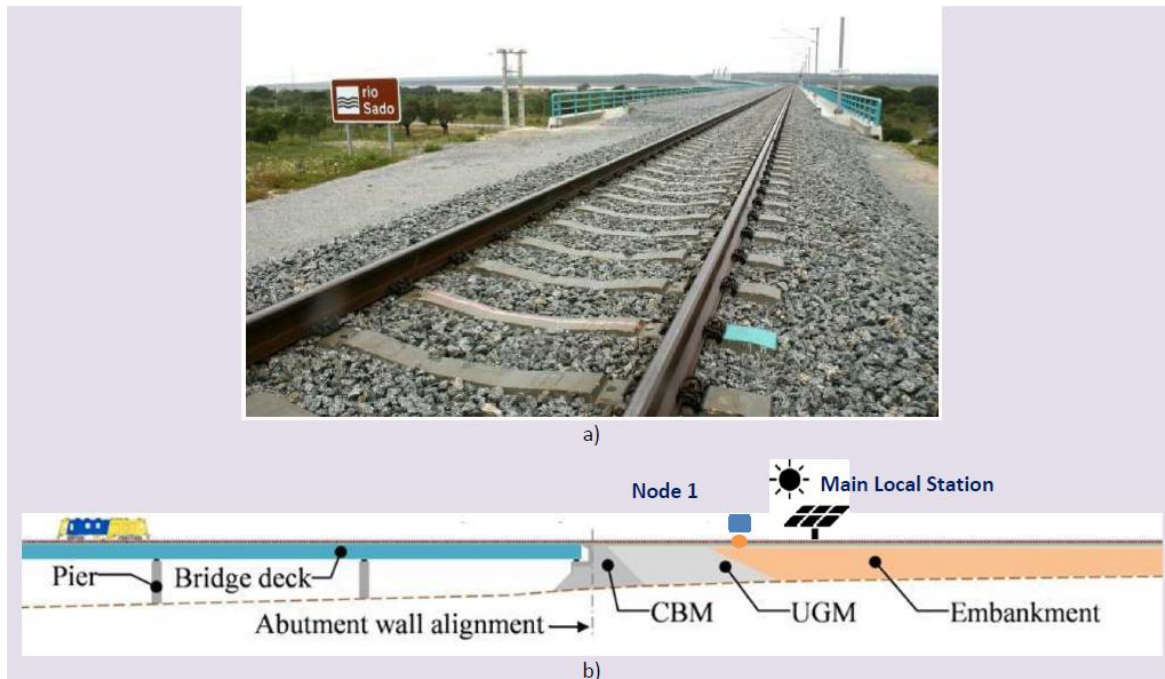


FIGURE 13. SOUTH ACCESS VIADUCT ILLUSTRATION A) AND LATERAL SCHEME B)

The sensor node (Node 1 of Zone 2) includes an energy harvesting module, a wireless Power transceiver module, a microcontroller and wireless transceiver, a MEMS accelerometer, a battery and a solar panel, Figure 24. All the modules and the sensor were inserted into a small box (125 x 85 x 55 mm) glued on one end of the sleeper. The wireless power receiver antenna stay outside the box as it can be seen in Figure 14 a).

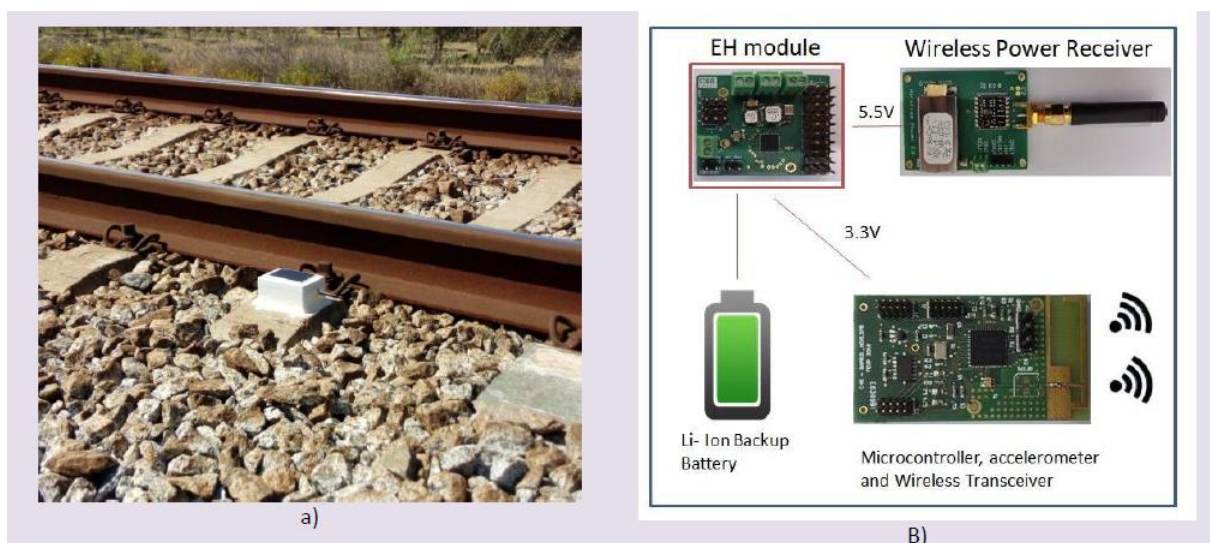


FIGURE 14. SENSOR NODE 1 INSTALLATION A) AND SCHEME B) AT ZONE 2

The accelerometer sensor was triggered by the vibrations on the sleeper and samples the data as the train passes over. The energy harvesting unit was also capable of receiving power from different types of local sources but here is mainly energy was provided by wireless power transmission using an RF antenna installed on the main local station.

The main local station was installed in a concrete base placed on the trackside platform at 4 meters from the nearest rail and the same alignment of the Node 1. In the same way as in zone 1, an equal metal structure was developed to hold a solar panel (130W, 1300x655mm) and an industrial enclosure (500x700mm ABS IP65). Here, the base and the pole were fixed to concrete base, Figure 25.



FIGURE 15. MAIN LOCAL STATION ILLUSTRATION AT ZONE 2

The main local station components are a minicomputer, a node data receiver, a 3G/4G router, a charge controller, a solar panel, 2 batteries, a RF power transmitter and other auxiliary accessories. Figure 26 shows the system scheme and installation illustration.

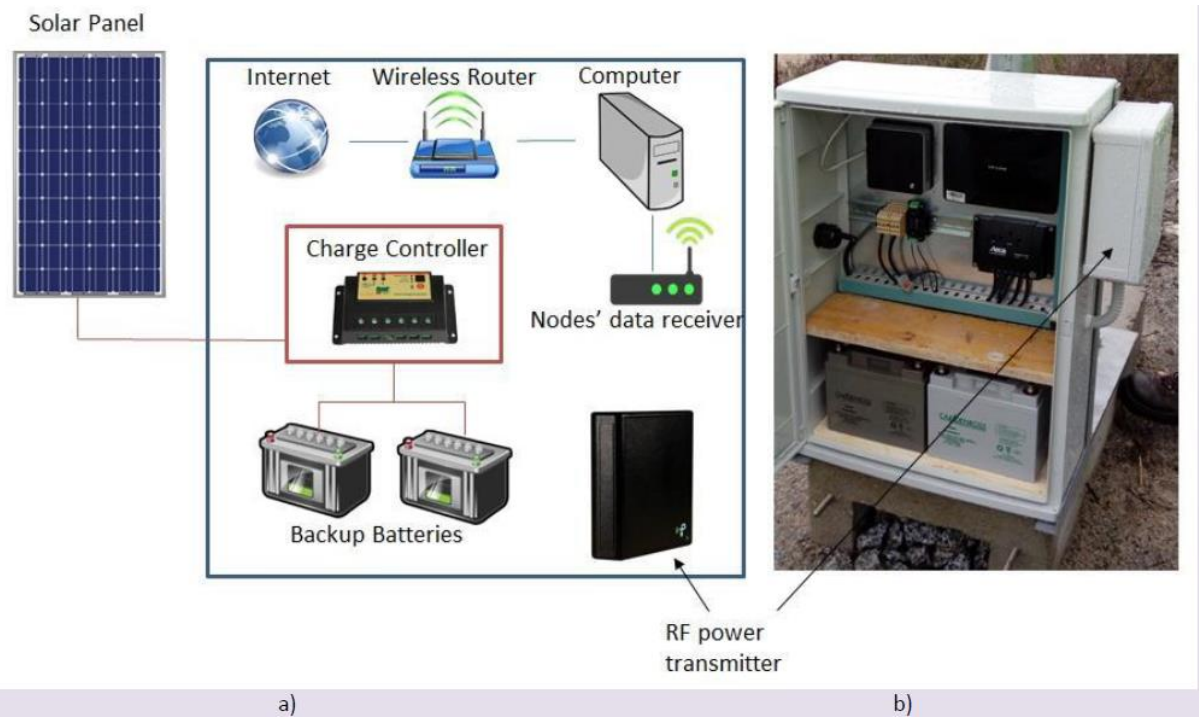


FIGURE 16. MAIN LOCAL STATION AT ZONE 2 SCHEME A) AND ILLUSTRATION B)

The RF power transmitter module was inserted in a box fixed to the industrial enclosure and vertically aligned with the sleeper. The receiver node collects the data from node 1 and saves in a database on the computer which can be accessed via internet. In Figure 17 shows the sensor installation location (FEUP Node 1) and the nodes from University of Birmingham that use the same box power.



FIGURE 17. SENSORS DISTRIBUTED IN THE TRANSITION

Positioning of track geometry signal

Without correct positioning of the track geometry signals, the monitoring activities such identifying faults, diagnosing the cause of defects and following the growing of the faults in time are really hard for track maintenance managers. Track assets have key roles to defining track geometry defaults. While the recording train is passing on the assets such Switch and Crossing, bridge, culvert and curve, there is unexpected change on the track geometry signals. This change can be over defined limits so can be seen as a defect. This kind of changes must be removed in the defect list. To do this, the positioning of track geometry signal must match with the real track layout to renew the defect list. Therefore, the position errors must be minimized for reliable monitoring.

According to Watson et al (2015), two main measurement systems; tachometer and odometer are used in the recording train to obtain train position. The tachometer measures the speed of the train on the other hand the odometer gives the distance travelled. The both system is mounted on the unpowered wheel and they measure wheel rotation speed and rotation number. When comparing these two systems, the odometers provide more precise position. The current odometer technologies give demanded accuracy at high service speed.

However, it is met with sort of problems while measuring position. Watson et al (2015) state this problem as wheel slip and slide, changing wheel diameter, varying rolling radius etc. It is very hard to eliminate these problems but they are kept in acceptable level.

To determine correct position, track assets such as the S&C, bridge, curve, cant profile etc. can be used by track maintenance managers. For example, if the rail profile is measured by the inspection systems, the S&C sections on the track provides good position estimation. There is clear difference between crossing and switching sections and normal rail profile.

In this work, the correct position is estimated in S&C section by using measured rail profile data as mention below.

The estimation is made on the rail profile data of the Izmit Station track section between 90+300km and 90+600 km which is carried out in May 2017. The S&C number of 31 is placed in this section and the design kilometre is 90+453 km in **Erreur ! Source du renvoi introuvable..**

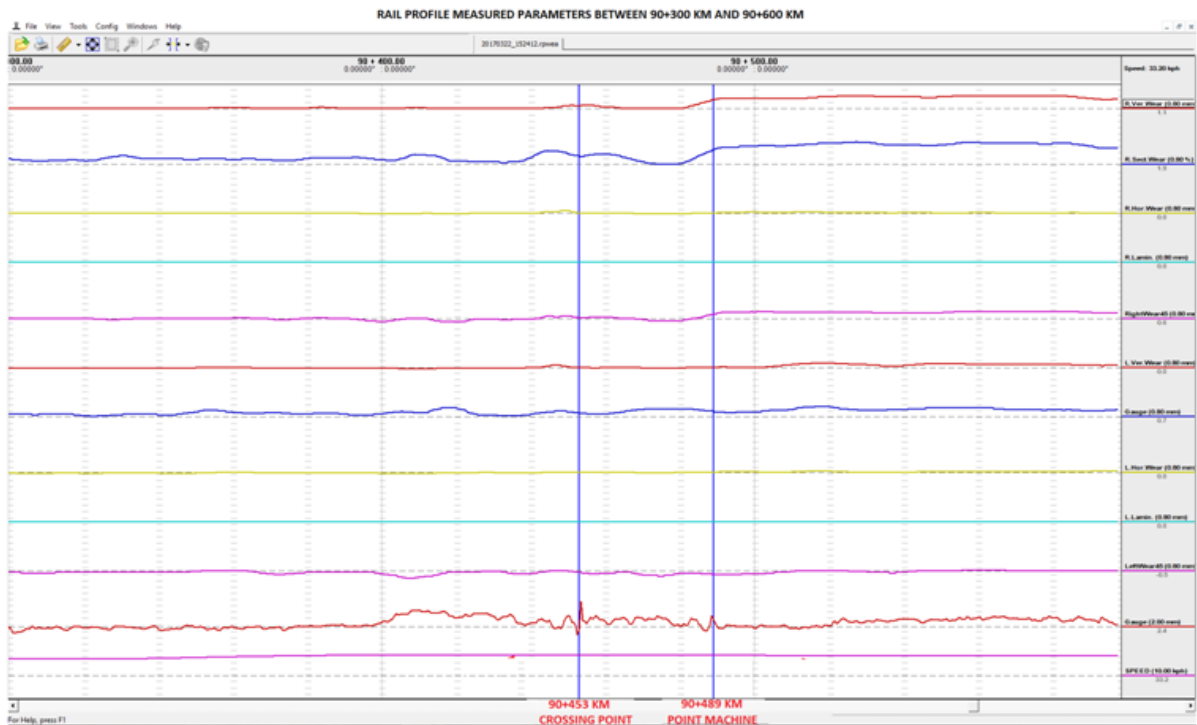


FIGURE 18. RAIL PROFILE MODEL

If this position is checked in rail profile data, it is seen that there is significant difference in the rail profile model which is shown in **Erreur ! Source du renvoi introuvable.** The blue line is measured profile and red one is ideal profile. When considering the blue line, it can be said that there is connection between two different model rails. This kind of connection on the S&C section can be placed only switch and crossing section. While the wing rail and swing nose crossing rail are contacting each other on the crossing section, on the switch section the blades rail and stock rail are contacting. When looking the model, it can be easily defined this area as the crossing section.

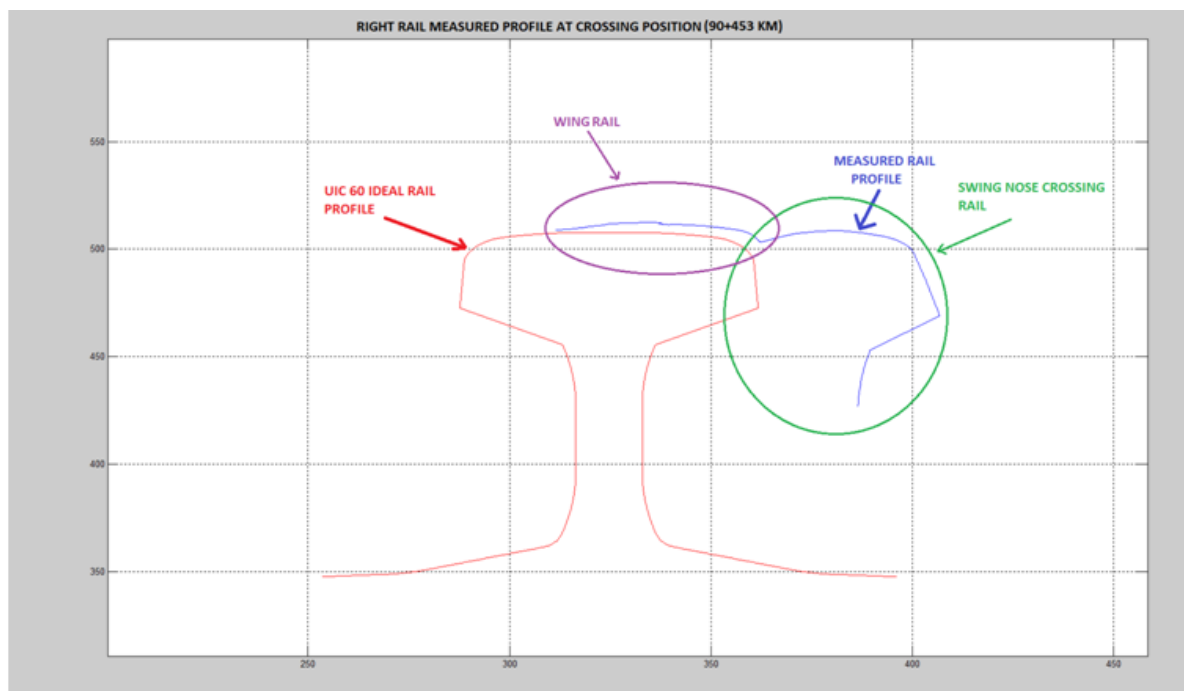


FIGURE 5.19 CROSSING SECTION 90+453 KM (AUTHOR)

Same approach is applied on the point machine section the design kilometre is 90+489 m in **Erreur ! Source du renvoi introuvable..** The measured rail profile is given in **Erreur ! Source du renvoi introuvable..** The measured rail profile data shows the connection between stock rail and blade rail. This information proves that the point machine is placed on chosen point.

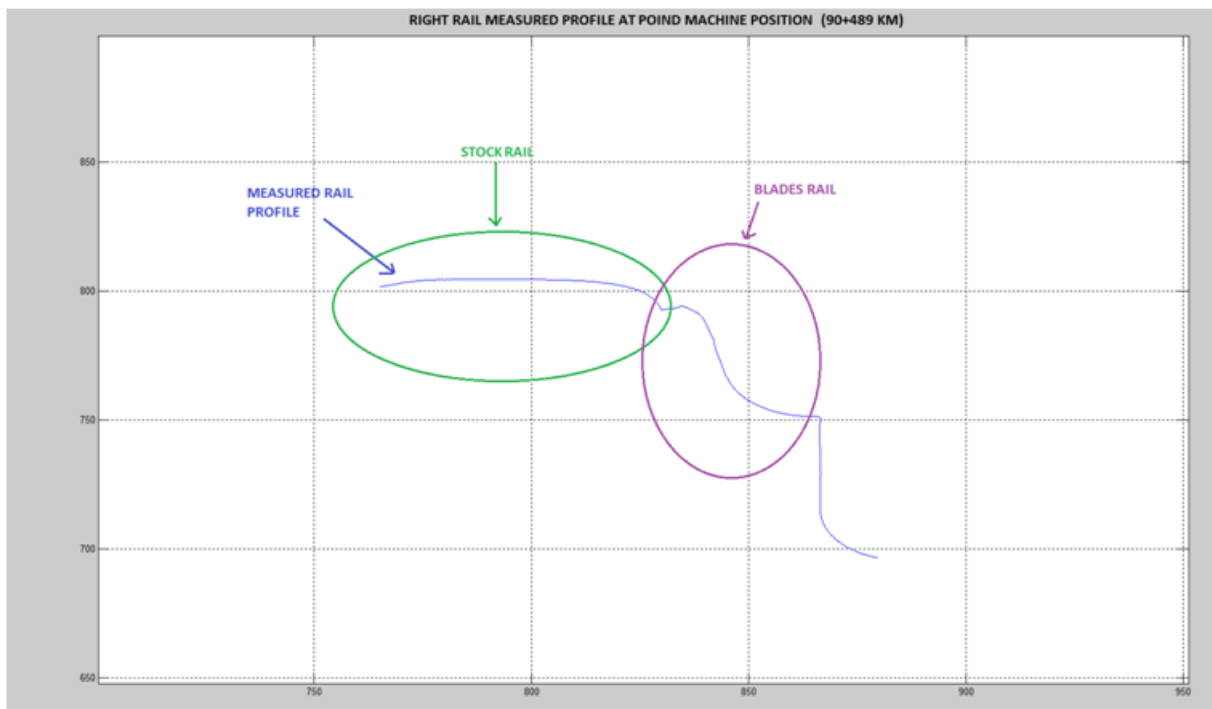


FIGURE 5.20 POINT MACHINE SECTION 90+489 KM (AUTHOR)

Another approach for determining correct position is train accelerations models on track assets. While train is passing on the S&C section, the instantaneous accelerations are generated on the axle boxes, bogies and coaches. These accelerations can be modelled for the S&C section and then the point machine and crossing section rail positions can be found.

The Piri Reis has Vehicle Dynamic Measurement System. This system records vertical and horizontal accelerations on bogie, axle boxes, and coaches via using accelerometers.

The Vehicle Dynamic Measurement System data for the Izmit Station track section between 90+300km and 90+600 km which is carried out in May 2017 is given **Erreur ! Source du renvoi introuvable..**

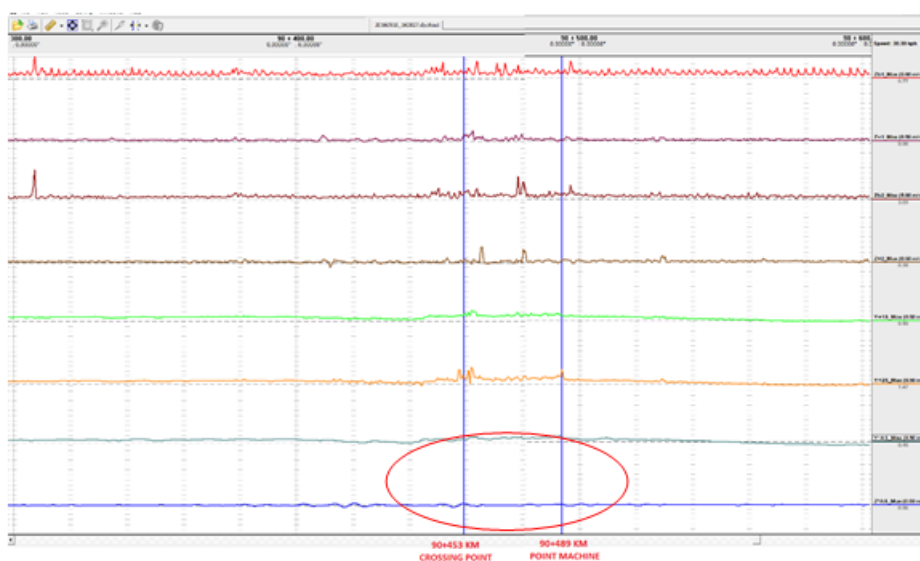


FIGURE 5.22 VEHICLE DYNAMICS PARAMETERS GRAPH THE SECTION BETWEEN 90+300KM AND 90+600KM (AUTHOR)

When considering results, the point machine and crossing point can precisely be found in the rail profile data. Then, this points use in the track geometry data to determine for correct positioning in **Erreur ! Source du renvoi introuvable.** For this measurement the positioning precise is very good. It is almost zero position error at chosen S&C section.

Consequently, the positioning errors in track geometry data can be eliminated and more reliable validation process can be obtained.

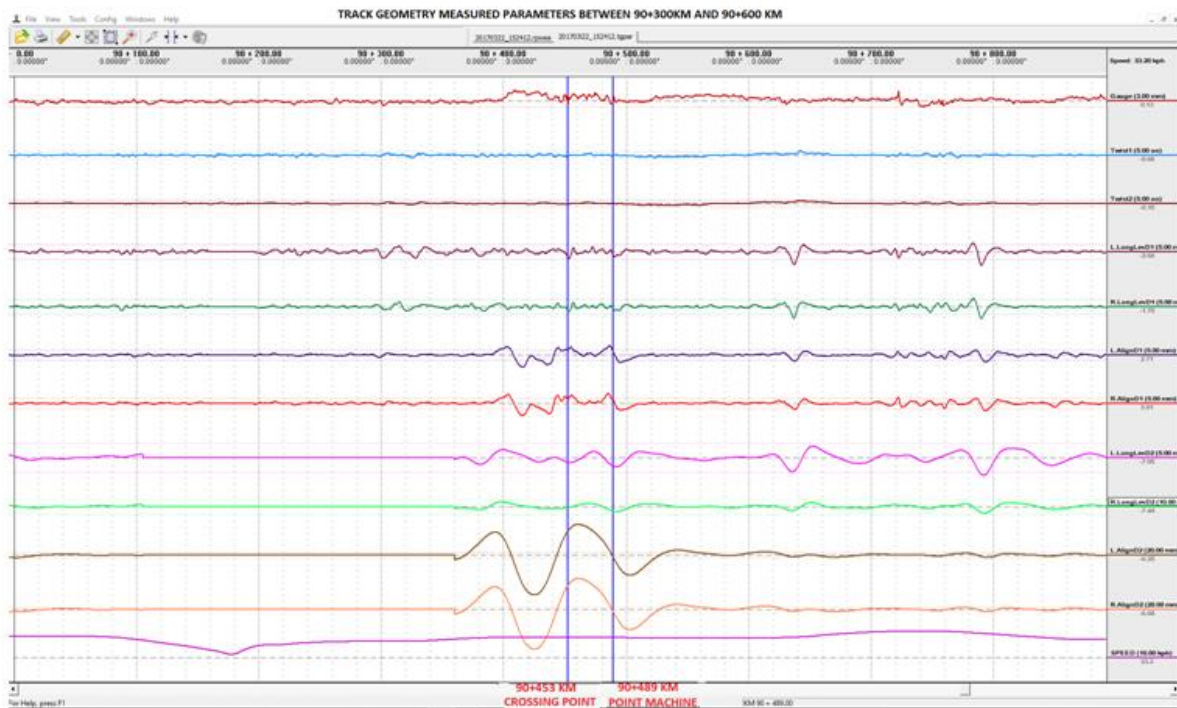


FIGURE 5.23 TRACK GEOMETRY PARAMETERS GRAPH THE SECTION BETWEEN 90+300KM AND 90+600KM (AUTHOR)

3.3. NEW CROSSING MATERIAL

A significant proportion of S&C for railway systems are currently manufactured from cast austenitic-manganese steel (AMS). AMS has traditionally been used owing to its good resistance to abrasion, high work hardening capacity on impact and excellent toughness following solution treatment and water quenching. The primary reason is the rapid work hardening rate that results in high hardness and the associated increase in resistance to wear. Without the rapid work hardening, resistance to abrasion, wear, and plastic deformation of AMS is poor. The nominal chemical analysis of AMS is 1.2% C, 13% Mn, 0.5%Si, which produces bulk hardness in the region of 200 to 250 HB. Following the passage of several MGT of traffic AMS S&C can reach hardness levels of 500 to 550 HB. However, there are a number of drawbacks with the use of AMS, which has prompted S&C suppliers to explore the use of alternative materials.

AMS is not an easy material to cast or machine into complex shapes needed for switches and crossings. The narrow freezing range of AMS results in many cavity type defects. Casting defects are common and are often the starting point of cracking seen in service. The presence of sub-surface casting cavities also increases the difficulty of weld restoration. Thus, the presence of such cavities restricts the permissible magnitude of vertical wear.

The new CogXmaterial and its implementation developed by Vossloh Cogifer is different than existing steel grades (e.g. CrBainit [DB], B320, B360, Mn-Mo) and will offer significant benefits over traditional

cast manganese crossings in terms of improved internal quality and the resulting extension to component life at the same time as reduced maintenance cost.

Thanks to its mixed metallurgical structure, the CogX material presents a high initial hardness and a high toughness.

The objectives of these demonstrators are to reach a TRL level of 5 and by field test evaluate the product.

Expected behaviour of CogX

The initial hardness is much higher for CogX material than for AMS steel, and a work hardening effect will occur in service (>550HB).

The CogX steel presents a high resistance to surface crushing and distortion thus improving transfer zone stability. For standard condition, no cracks should appear on the running surface.

Hard track conditions may nevertheless allow micro-cracks appear on the running surface in the transfer area. In such case, propagation is not expected thanks to the structure of the material.

The CogX material is repairable in track when necessary using standard surface preparation, control and arc weld refurbishing.

CogX demonstrator

The target of the demonstrator is to confirm the effects that can indeed be avoided through the use of the proposed new CogX material, and to quantify the resulting decrease in whole life costs.

The Demonstrator is a crossing manufactured in the new CogX steel that replaced an existing 60E1 crossing (EV-UIC60-500-1:12; Turnout TG 1/12 R500 m) manufactured from cast manganese.

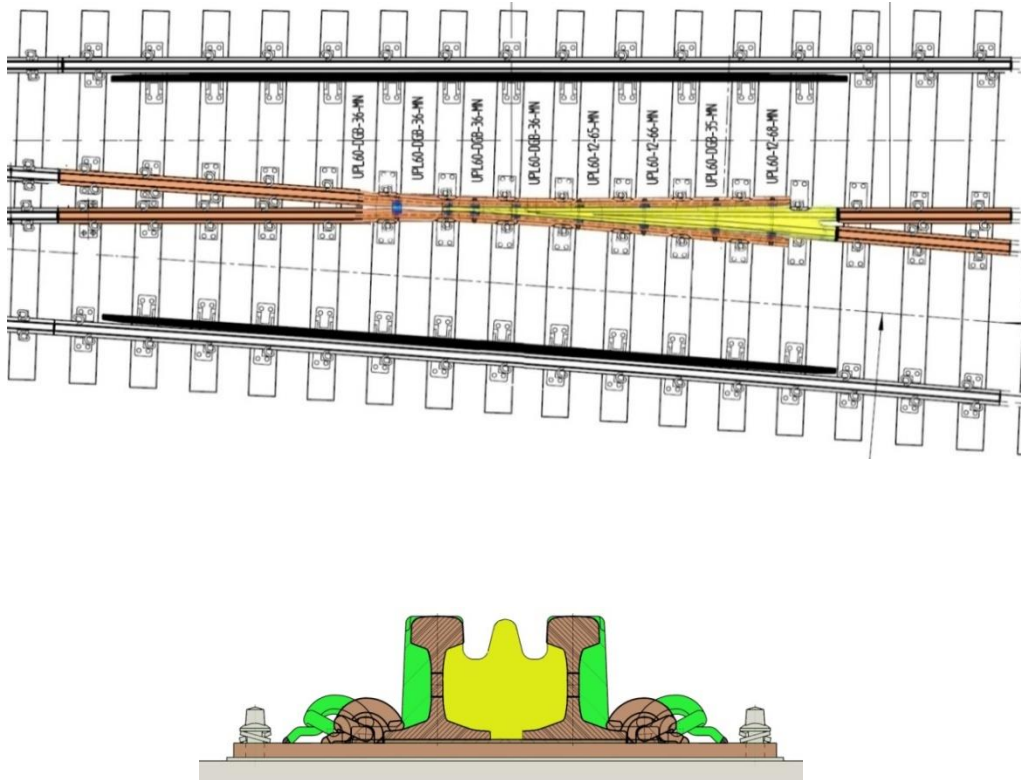


FIGURE 24. DEMONSTRATOR CROSSING

Same geometry and compatible baseplates (8 special provided with the test crossing). CogX material is implemented on the crossing point and represented in yellow on the drawing. The green section represents the monoblocMn crossing shape replaced by the rails and point. The fasteners (Pandrol clip) are moved in order to be close to the rail. The baseplate has same holes as for Mn crossing, but adapted shoulders.

The demonstrator crossing was installed in Sweden near Göteborg (Kungsbacka station, see Figure 25.) on 3rd August 2017. In Kungsbacka 36 trains/day goes south and the yearly load is 5.7 MGT/year. The installation was done within a time slot of 3 ½ hour.

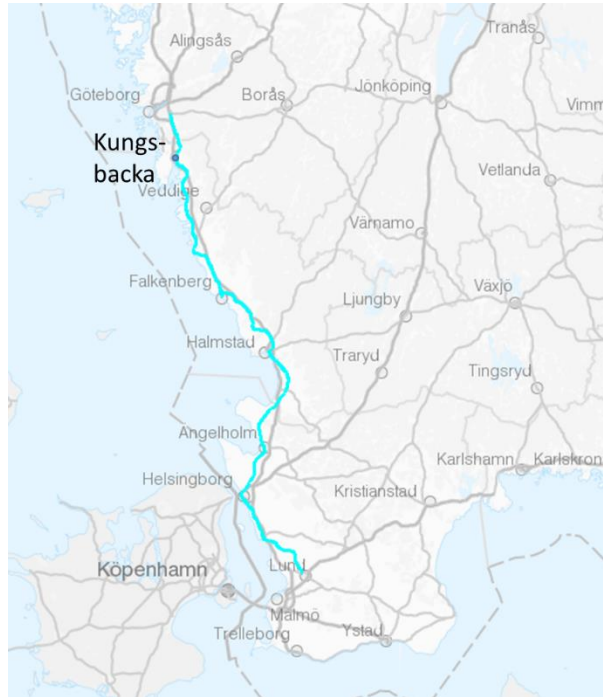


FIGURE 25. KUNGSBACKA, A STATION ON THE WESTCOAST LINE

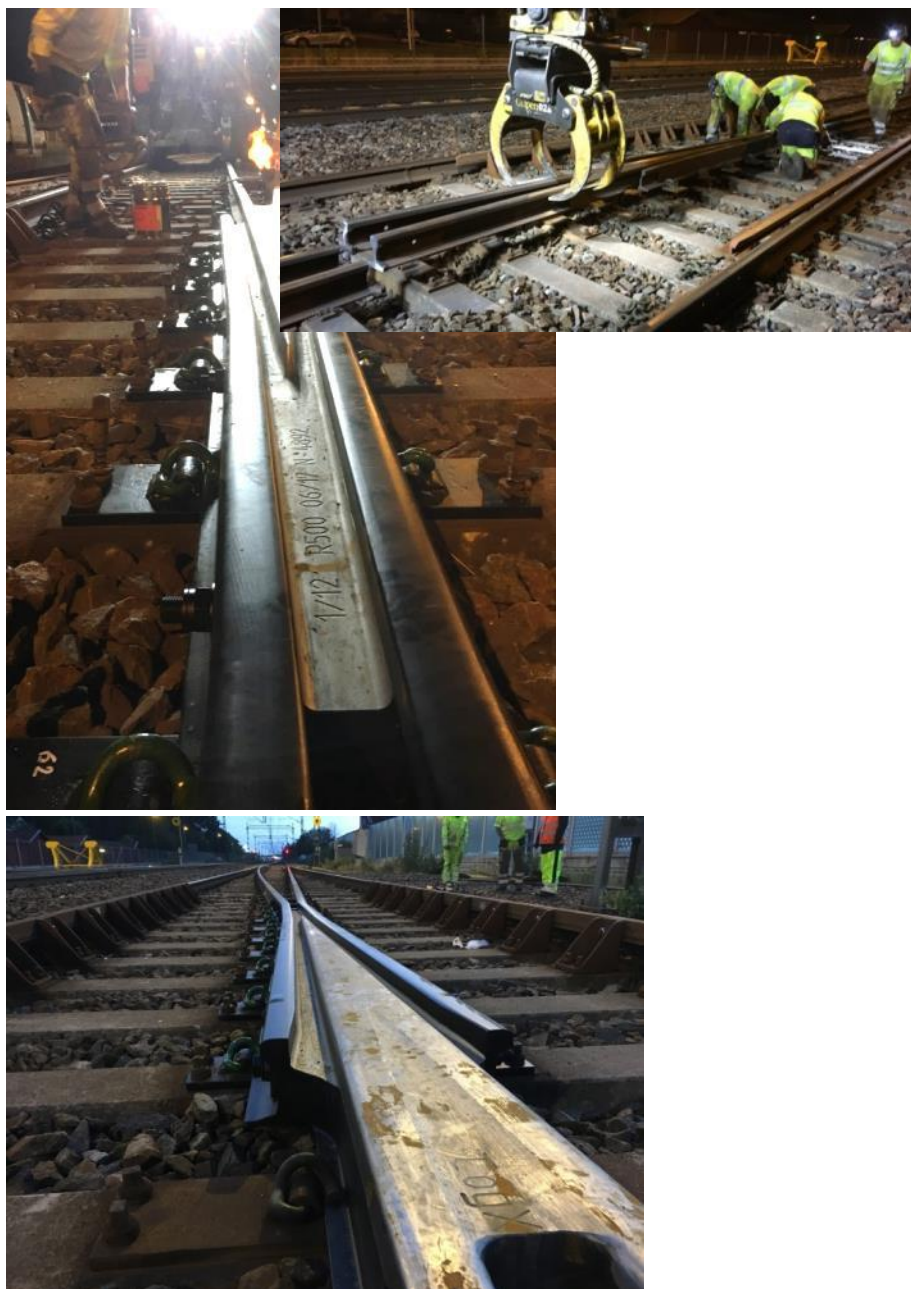


FIGURE 26. COGX-CROSSING AFTER INSTALLATION IN KUNGSBACKA (SWEDEN)

Results

The first inspection was done on 4th September 2017 after 1 month traffic (0.5MGT). Visual inspection, 3D-scan, dye-penetration showed that the condition was good and no problem was found. Hardness test showed an expected increase in hardness.



FIGURE 27. TOP VIEW OF THE TRANSFER AREA

No damage or plastic deformation is detected on the CogX point of frog, nor on the two flash butt welds with the rail, nor on the wing rails. The transfer conditions can be qualified as good.



FIGURE 28. DETAIL OF THE CROSSING NOSE



FIGURE 29. DETAIL OF THE RUNNING SURFACE OVER WELD A – DIRECT LINE

3D laser measurements done with HANDY SCAN700 on transfer area. In 30 is shown the targets that are used to help the scanner to compensate for the movement during the measurement. The accuracy according to the vendor is 0.03 mm with an angle-drift of 0.06 mm per meter. That is an accuracy of 0.06 mm should be possible on a length of 0.6 m.

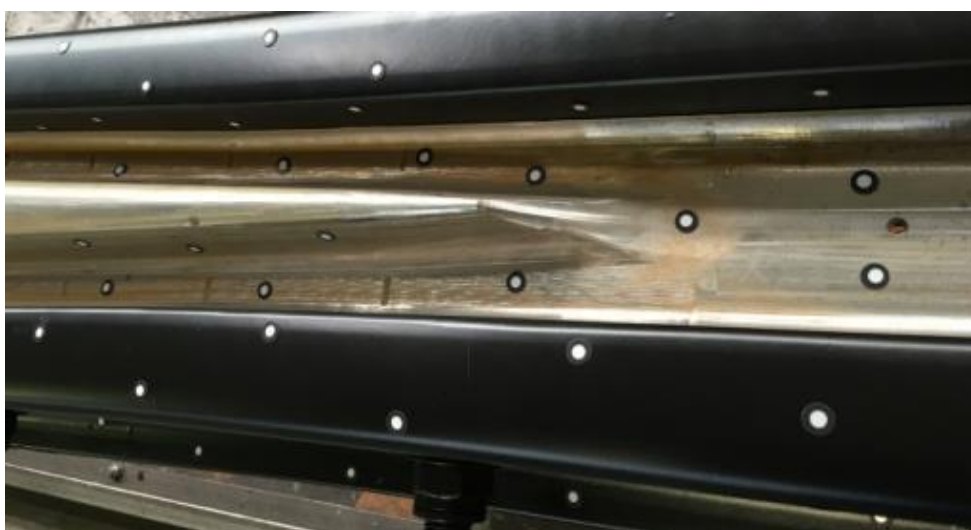


FIGURE 30. SMALL TARGETS ARE PLACED ON THE SURFACE TO ENABLE A 3D-SCANNING

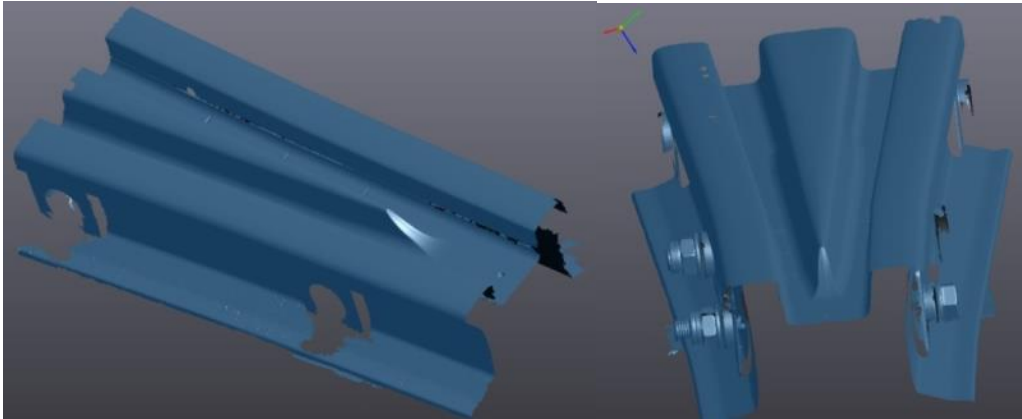


FIGURE 31. RESULT FROM 3D-SCANNING

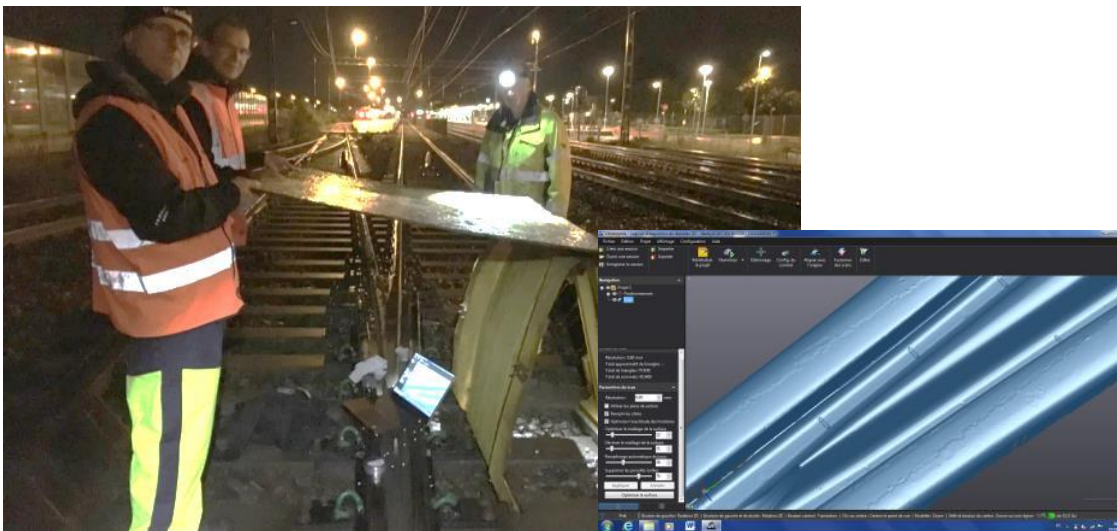


FIGURE 32. AS IT RAINED THE MEASURED AREA WAS COVERED DURING 3D-SCANNING AND DYE-PENETRATE TESTING

Figure 33 shows a comparison with the initial geometry and after 5 weeks in field. To improve accuracy the 3D scanner uses small targets as references, which are shown as holes in the figure. To take a measurement 5 of the targets should be visible at all time during the scanning. The measurement shows that the paint, which was on the wing rail, has been removed in the running area on both sides (blue colour in the figure), and this loss is in the order of 0.25-0.30 mm. There is no wear detected yet on the CogX point (difference < 0.1mm).

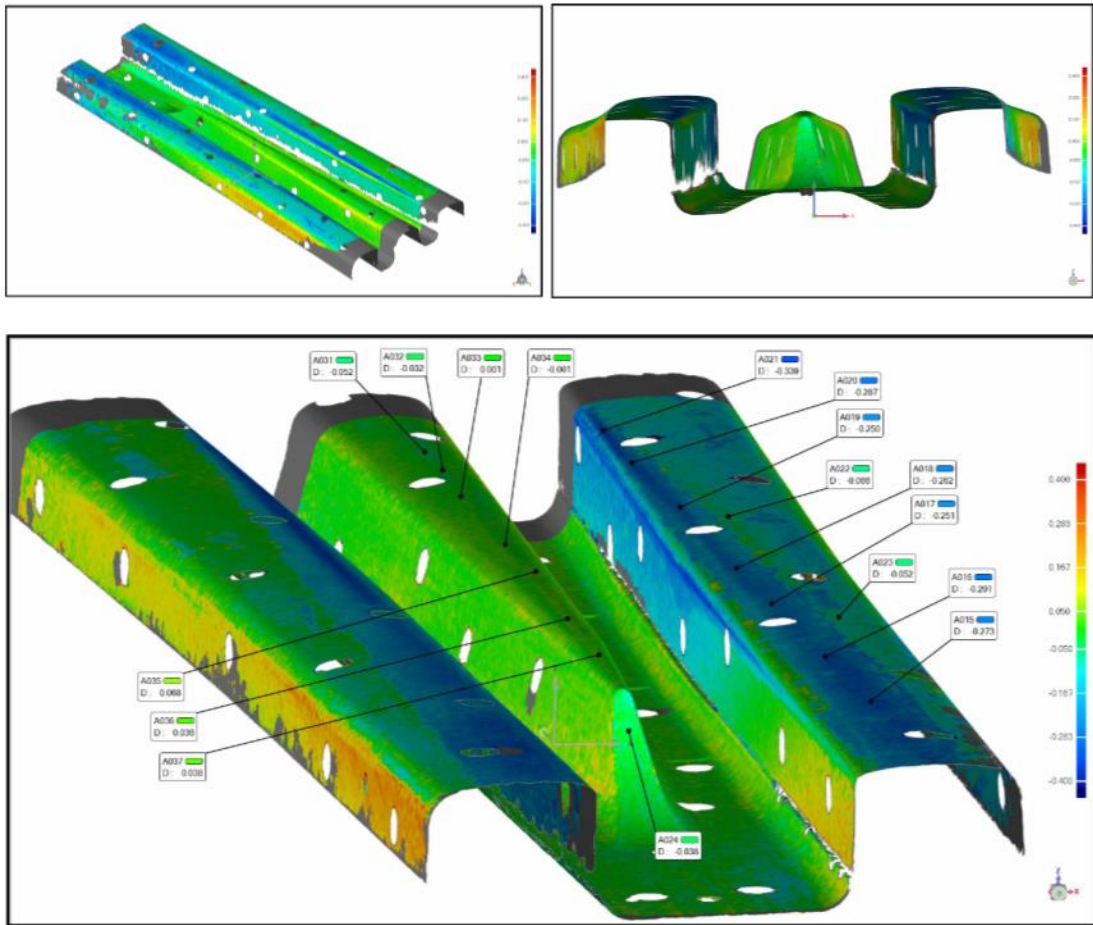


FIGURE 33. COMPARISON BETWEEN INITIAL SCANNING AND SCANNING AFTER 5 WEEKS IN FIELD

Dye penetrant testing

The extent of the dye penetrant testing has been limited at the transfer area and the running surface over the flash butt welds. After developer application, no indication has been detected, nor on the CogX point nor on the welds.

Hardness

The hardness tests have been performed on the CogX point and R350HT wing rails with KrautkramerDynapocket device to see the hardness evolution in relation with MGT.

AVERAGE HARDNESS EVOLUTION ON THE COGX POINT

| MGT | Average hardness on CogX point (HB) |
|-----|-------------------------------------|
| 0 | 474 |
| 0,5 | 498 |
| ... | >550 expected |

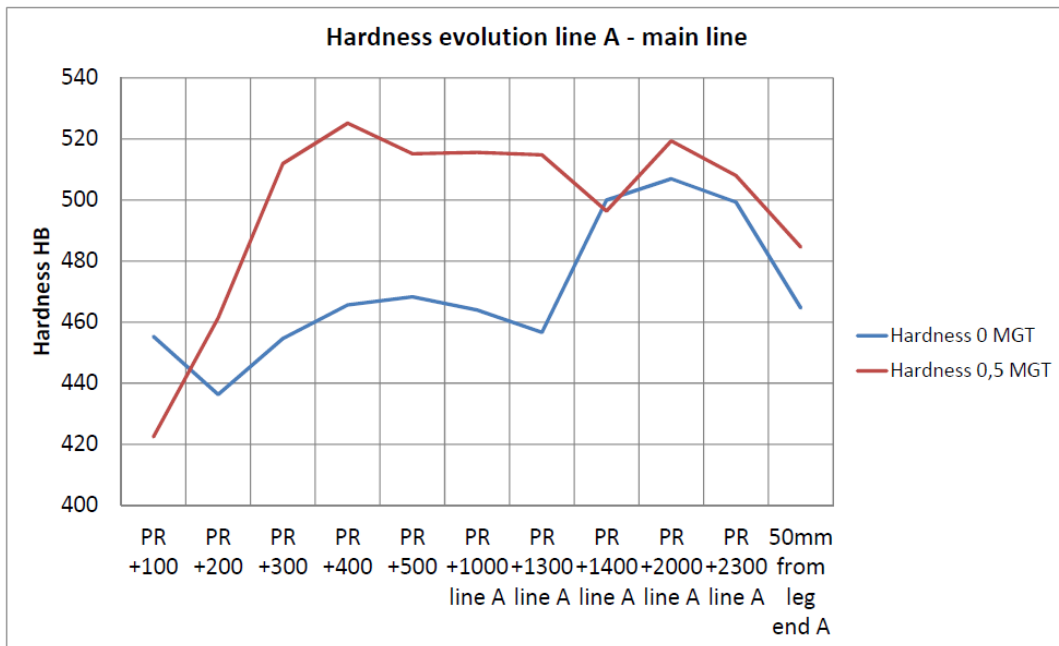


FIGURE34. HARDNESS EVOLUTION IN RELATION WITH THE RELATIVE POSITION TO PR (REAL CROSSING POINT)

The expected work hardening effect on the hardness has confirmed even early stage.

3.4 DATA COLLECTION DURING IN-SITU TEST CAMPAIGNS

The general goal of the two in-situ campaigns was to create a data base of the vibrations measured in a real track produced by passing-by of different trains travelling at high speeds (around 300 km/h) and its dynamic behaviour. This data base will be used as a source to validate the test results obtained in CEDEX Track Box (CTB). To make easier the comparison, the instrumentation set used in the second campaign reproduced a typical configuration used in CTB.

DESCRIPTION OF THE WORKS

The first campaign was performed by CEDEX on November, 2015 at PK 72+200 of the Madrid-Barcelona High Speed Line, while the second one carried out on June, 2016 at PK 74+233, a straight track section far from stations, tunnels and bridges, in which trains can travel at their maximum speed in this line (300 km/h).

Figure 4 shows a photograph of the test site of the second campaign.



FIGURE 35: PK 74+233 MADRID-BARCELONA HIGH SPEED LINE- STRAIGHT TRACK SECTION

More details about these in-situ campaigns can be found in Appendix 8.2.of D11.2

The instrumentation installed, that can be seen in Figure 5, consisted of the following sensors to be used with techniques developed by CEDEX [3 and 4]:

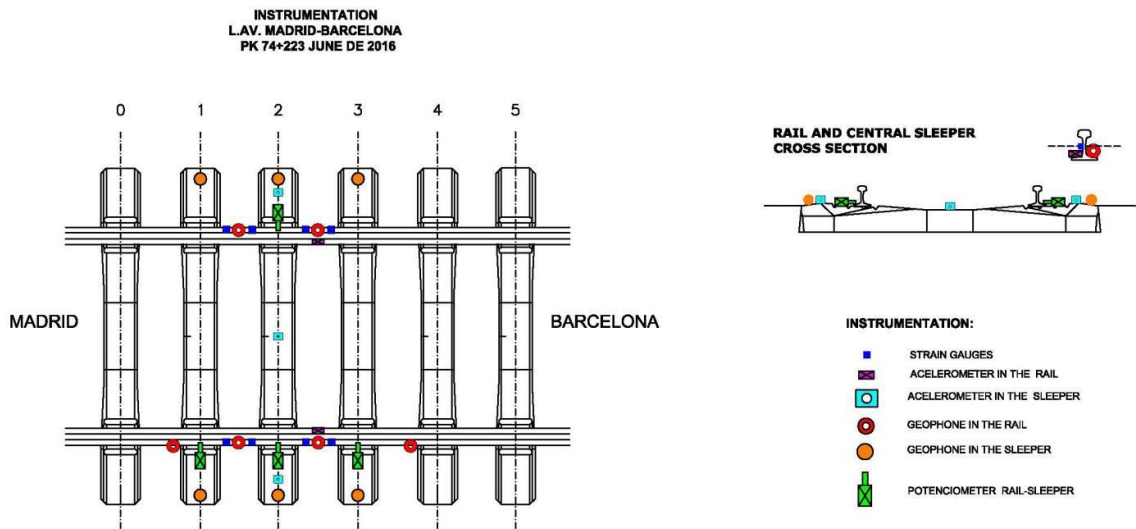


FIGURE 36. SKETCH OF THE INSTRUMENTATION INSTALLED FOR THE SECOND CAMPAIGN

- Eight strain gauges (represented by dark-blue squares): the gauges are glued at the level of the neutral fibre of the rail in order to measure only shear strains. Loads are obtained using the pair placed at the span between two sleepers.
- Seven 2 Hz geophones installed in the rail (marked with red spots): they are used to measure the vertical velocity of the vibration in the rail produced by the trains pass-by. It is also possible to obtain the rail deflections by integrating these velocity signals.
- Six 1 Hz geophones (represented by orange circles): they are stacked at both ends of the sleeper surface to measure the vertical velocity of the vibration at those points.
- Two vertical accelerometers stacked in the rail (shown with fuchsia rectangles).
- Three triaxial accelerometers stacked in the sleeper surface (represented by light-blue squares).
- Four potentiometers (presented with green rectangles): they are used to measure the railsleeper relative motion, from which is possible to calculate the pad deformation. Furthermore, six ballast particles instrumented with accelerometers were placed in different positions.

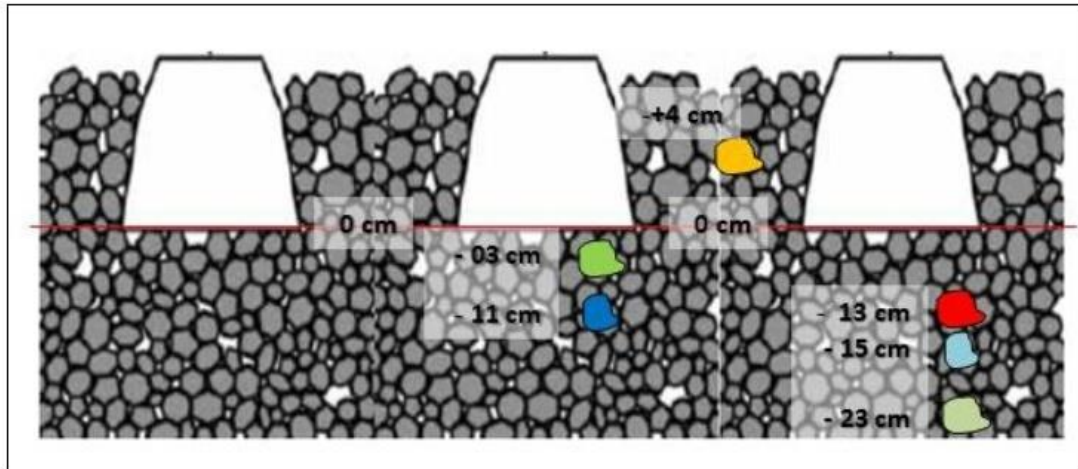


FIGURE 37. POSITION OF THE BALLAST PARTICLES INSTRUMENTED WITH ACCELEROMETERS

A total of 8 and 37 trains were recorded, respectively, in the first and second campaigns. Those trains covered five types of trains (Talgo S102, Siemens S-103, CAF S-120, Talgo AVRIL) that travel at speeds between 225 and 310 km/h.

The following step is the process of the raw data for each kind of sensor. For all the time signals obtained, the first step is to calculate the Fast Fourier Transform (FFT) to visualize the frequency domain and then to decide the filter which must be applied, in case it is necessary. In general for this kind of studies, the most used filter is the Low Pass Filter (LPF) which cuts off frequencies above the range of interest in each particular case.

RESULTS

The parameters that have been analysed are the following:

- Track stiffness, considered as the ratio between the loads applied by the train, obtained from the strain gauges, and the rail deflection obtained from the time integration of rail velocity.
- Pad vertical displacement, measured by potentiometers as the relative motion between rail and sleepers.
- Vertical rail velocity.
- Vertical sleeper velocity.
- Vertical rail acceleration
- Vertical sleeper acceleration
- Ballast particle acceleration.

More details about the results obtained in these two in-situ campaigns can be found in Appendix 8.2.D12.1

3.5. INNOVATIVE DESIGNS AND METHODS OF STRUCTURES ON VERY HIGH SPEED LINES.

Deliverable D12.3 presents important aspects of railway bridge dynamics for very high speed lines. The different demonstrators on infrastructure are:

Case Study 1- PORTAL FRAME BRIDGE

The first case study is a portal frame bridge at Orrvik, Figure 13, located along the Bothnia Line in Sweden. Based on the simple 2D-model, a peak acceleration of 6.0 m/s² was calculated at a critical train speed of 286 km/h. The span length is 15.2 m and the first natural frequency was calculated to 5.9 Hz. Experimental results from passing trains are reported in [24], but no clear information on the natural frequencies or damping is presented.

The experiments were performed during high-speed tests with the Green Train. The speed record for the Green train is 303 km/h, but during the bridge test the highest speed was about 280 km/h.

Accelerometers were mounted on top of the edge beams, 1.5 m from mid-span. The peak acceleration during the train passages at different speeds are plotted in Figure 14. The measured acceleration is subjected to a low-pass filter at first 90 Hz and the 30 Hz. A 2D frame model proposed by [24] shows overall reasonable agreement for the case of 90 Hz frequency range. The acceleration magnitude is decreased significantly when using a 30 Hz filter.



FIGURE 38. THE PORTAL FRAME BRIDGE AT ORRVIK.

Case Study 2- STEEL CONCRETE COMPOSITE BRIDGE

The second case study is a 36 m simply supported single track steel-concrete composite bridge, at Skidträsk, about 190 km North of Umeå. The bridge is designed for freight trains with 25 tonnes/axle

but not for high-speed trains. A long-term monitoring system was installed for continuous monitoring of deck acceleration and strain in the steel beams.



FIGURE 39. THE PORTAL FRAME BRIDGE AT SKIDTRÄSK

A 3D FE-model was developed, including relevant SSI components from both the ballasted track and the substructure. Distribution functions for the variation of concrete stiffness, ballast stiffness and foundation stiffness was assumed and a Bayesian model update technique was used to find plausible matches between the model and the experimental data. The results showed that the change in vertical bending frequency is mainly governed by the foundation stiffness, whereas the change in torsional frequency is mainly governed by the ballast stiffness. The model proposed that the Emodulus of the ballast would increase from 180 MPa in the summer to 1500 MPa in the winter. The corresponding increase in the foundation was from 75 MPa to 110 MPa. The model did not propose any change in E-modulus for the concrete.

The response from passing trains on the same bridge is presented in [23]. Based on the measured free vibrations after train passages, a change in both natural frequency and damping was observed. The ballasted track was believed to be the main source of this non-linear behaviour. Later studies of the mechanism of bearings [21] do however suggest that the hysteresis behaviour of roller bearings may have a significant impact in the response of the bridge. For low amplitude vibrations, the roller bearings are expected to act as fixed.

Case Study 3- SOIL STEEL COMPOSITE BRIDGE

The third case study is a corrugated steel culvert in Märsta, about 40 km North of Stockholm. Corrugated steel culverts are statically designed accounting for composite action with the surrounding soil but its performance during dynamic loading is not readily known. The studied bridge serves as a

pedestrian underpass, Figure 17, and has an elliptical section with a horizontal diameter of 3.75 m and a vertical diameter of 4.15 m. The fill height at the crown is about 1.9 m and carried two tracks. The line consists of mixed train traffic with both medium heavy freight trains (max 22.5 tonnes/axle) and various commuter and long distance train (with speeds up to 170 km/h).



FIGURE 40. THE SOIL-STEEL COMPOSITE BRIDGE AT MÄRSTA DURING PASSAGE OF AN X52 TRAIN, REPRODUCED FROM

The bridge was instrumented with displacement transducers, accelerometers and strain gauges. The main aim of the measurements was to gain further understanding of the dynamic behaviour during train passages and if they would be suitable for HSR. A small part of the instrumentation is shown in Figure 18.

The peak acceleration from a number of passing trains is shown in Figure 19, after applying a 30 Hz low-pass filter. For conventional slab-like bridges, the vertical deck acceleration is an indirect measure of the allowable vibration of the track. It is therefore of interest to investigate the relation between the acceleration of the steel pipe to the acceleration in the track zone. Train model X52, similar to the Green Train, pass the bridge at about 170 km/h in most cases. The acceleration a_1 in the steel pipe appears well correlated to the acceleration a_2 at the ballast shoulder. Acceleration a_3 in the ballast within the track zone does however scatter significantly. Values with $a_{max} < 0.4 \text{ m/s}^2$ is due to trains passing on the opposite track.

Case study 4 – MULTI- SPAN CONCRETE SLAB BRIDGE

The last case study comprise controlled excitation of a three-span two track concrete bridge in Södertälje, 35 km South of Stockholm. The side spans are 11.1 m and the mid-span 18.4 m. The bridge

was part of the feasibility study reported. From the simplified 2D analysis, excessive accelerations were predicted, owing to the integrated back-walls with 3.0 m over-sail.

A hydraulic bridge exciter has recently been developed by KTH (as part of the IP2-In2Track European project) and the presented bridge serves as a first full-scale pilot test. The concept of the hydraulic exciter is to apply a constant amplitude load with variable frequency at the bridge soffit. Testing can therefore be performed without closing the track and the mass of the exciter equipment does not influence the bridge response. The system essentially consists of a support plate, a hydraulic load cylinder and a truss frame that is pre-stressed against the bridge soffit. A photo of the system when installed on the bridge is shown in Figure 22. The force is monitored by a load cell at the upper connection to the bridge and an MTS FlexTest SE controller assures that constant load amplitude is achieved. The system is able to account for flexibility in both the test frame and the foundation. The load cylinder has a capacity of 50 kN. The system works in compression, enabling load amplitudes up to 25 kN. The system is designed for a working range up to 50 Hz, but can be increased for lower displacement amplitudes.

Although the load capacity is less than a conventional train axle load, the main advantage is that the excitation can be controlled in both load and frequency. The bridge exciter is expected to enable relatively high amplitude vibrations, since the steady-state response can be obtained. Further, experimental frequency response functions (FRF) can be obtained with high accuracy, serving as valuable input for model updating and structural identification. Further details on the bridge exciter and the pilot test are presented in [28] and [29].



FIGURE 41. THE BEAM BRIDGE AT PERSHAGEN.



FIGURE 42. THE BEAM BRIDGE AT PERSHAGEN, DURING TESTING WITH THE HYDRAULIC EXCITER

VERIFICATION BY FULL SCALE TEST- TEST ON VIADUCT PIO24

Ineco, Cedex and Adif performed full-scale tests in November 2015. The instrumentation consisted of accelerometers, strain gauges and displacement transducers. The response from passing trains was measured.

All details about this performance are in **Deliverable D12.3- Appendix A**

4. Conclusions

Monitoring use case (Alcácer do Sal Railway Bridge)

Without correct positioning of the track geometry signals, the monitoring activities such identifying faults, diagnosing the cause of defects and following the growing of the faults in time are really hard for track maintenance managers. Track assets have key roles to defining track geometry defaults. While the recording train is passing on the assets such Switch and Crossing, bridge, culvert and curve, there is unexpected change on the track geometry signals. This change can be over defined limits so can be seen as a defect. This kind of changes must be removed in the defect list. To do this, the positioning of track geometry signal must match with the real track layout to renew the defect list. Therefore, the position errors must be minimized for reliable monitoring.

Innovative designs and methods of structures on very high speed lines

In this report, different aspects of railway bridge dynamics have been presented and discussed. The success in predicting the real dynamic response highly depends on the choice of structural model. An increased level of detail may improve the results, but reliable input data for such models are not always available. On the other hand, simplified models may prove sufficient and sometimes with similar accuracy as far more complicated models, provided that the main governing features of the real response can be described.

The dynamic response of railway bridges on high-speed lines is limited by a set of serviceability criteria. Some of these, e.g. the vertical deck acceleration, may sometimes be over conservative. More accurate design limits may result in the use of slender bridges and enabling upgrading of more existing bridges to higher speeds, with a required safety limit.

Increased understanding of the real dynamic manner of action by experimental testing can hopefully result in more accurate predictions of the dynamic response and model updating and hence less need for safety margins in the models.

Some of the main conclusions drawn from this study are:

The analyses on short two-span and three-span beam bridges show that their dynamic behaviour need to be studied carefully in the speed range between high speeds (up to 350 km/h) and very high speeds (up to 480 km/h). Double-track two-span bridges, as well as single-track three-span bridges, may have acceleration levels above or close to the Eurocode acceleration limit 3.5m/s^2 for very high speeds.

The dynamic analysis on portal frame bridges shows:

- For closed frame bridges, the lower is the span length, the higher is the resonance risk for high speed. The vertical acceleration at mid span for 5m closed frame bridge is higher than acceleration for 10m closed frame bridge.
- For open frame bridges, the lower is the span length, the higher is the resonance risk for high speed. The vertical acceleration at mid span for 10m open frame bridge is higher than acceleration for 15m open frame bridge.
- The results of studied bridges are higher than limit of 3.5 m/s² for ballasted track or 5 m/s² for track without ballast. To respect these limitations for speed up to 480 km/h we have redesigned and increased the thickness of the deck.
- The effect of track irregularities was found to compare well with the Eurocode factor (1+0.5 ϕ''), for track irregularities corresponding to EN 13848-6 track quality class A.
- At the presence of track irregularities, significant high-frequency content was observed in the bridgedeck acceleration for some of the case study bridges. There is a need for further research on the behaviour of ballast at different frequencies of vibration in order to give thorough recommendations on the choice of cut-off frequency.
- The results of comfort analysis and track irregularities for portal frame bridges shows:
 - The passengers comfort does not govern the design of the bridges for small span bridges
 - Track irregularities create:
 - No increase of vertical deck acceleration
 - Large increase of vertical passenger acceleration
 - Moderate increase of transverse passenger acceleration.

5. References

- Einstein Z., Zweistein D., Dreistein V., Vierstein F. & St. Pierre E. : “Spatial integration in the temporal cortex.” *Res. Proc. neurophysiol Fanatic Soc.* 1, 45-52, 1974.
- Chou O. & Lai A.: “Note on the tomatic inhibition in the singing gorilla.” *Acta laryngol.* 8, 41-42, 1927.
- Perec G.: “Experimental demonstration of the tomatotropic organization in the Soprano (Cantatrix sopranica L.)”
- CEDEX Track Box as an experimental tool to test railway tracks at 1:1 scale. J. Estaire, F. Pardo de Santayana, V. Cuéllar. In Proceedings of the 19th International Conference on Soil Mechanics and Geotechnical Engineering, Seoul 2017.
- Testing railway tracks at 1:1 scale at CEDEX Track Box. José Estaire, Vicente Cuéllar & María Santana. International Congress on High-Speed Rail. Ciudad Real (Spain), 4-6 October 2017
- Instrumentation techniques for studying the horizontal behaviour of high-speed railways. J. Moreno Robles; I. Crespo-Chacón; J. L. García-de-la-Oliva. *Procedia Engineering - Advances in Transportation Geotechnics III.* 143, pp. 870 - 879. Elsevier, 2016.
- On the use of geophones in the low-frequency regime to study rail vibrations. I. Crespo-Chacón; J. L. García-de-la-Oliva; E. Santiago-Recuerda. *Procedia Engineering - Advances in Transportation Geotechnics III.* 143, pp. 782 - 794. Elsevier, 2016.
- Maciel, R. & Ferreira, P., 2016. Optimization algorithm applied to VHS track design towards enhanced track dynamic performance and reduced settlement, 11th World Congress on Railway Research -WCRR 2016. Milan.
- Ferreira, P. & López-Pita, A., 2015. Numerical modelling of high speed train/track system for the reduction of vibration levels and maintenance needs of railway tracks. *Construction and Building Materials*, pp. Volume 79, pages 14–21.
- Ferreira, P. & Maciel, R., 2014. Inverse problems applied to the optimization of numerical model validation of railway track dynamic behavior. Lisbon, 4th International Conference on Engineering Optimization - EngOpt2014, Lisbon, 8-11th September, 2014.
- Ferreira, P. & López-Pita, A., 2013. Numerical modeling of high-speed train/track system to assess track vibrations and settlement prediction. *Journal of Transportation Engineering*, Volume 139, pp. 330-337.
- Ferreira, P., 2010. Modelling and prediction of the dynamic behaviour of railway infrastructures at very high speeds, PhD Thesis, Instituto Superior Técnico, Lisbon.